Frontiers in Bioscience Landmark

Front. Biosci. (Landmark Ed) **2026**; 31(2): 48473
https://doi.org/10.31083/FBL48473

Original Research

Bevacizumab-Primed Vascular Normalization Enhances Intratumoral Delivery and Efficacy of the tBID-Armed Oncolytic Adenovirus KD01 in Glioma

Wei Gong[1], Baiwei Zhang[1], Zuodong Yuan[1], Chansachak Chea[1], Fei Ye[1,*]

[1]Department of Neurosurgery, Tongji Hospital, Tongji Medical School, Huazhong University of Sciences and Technology, 430030 Wuhan, Hubei, China
*Correspondence: feiye@tjh.tjmu.edu.cn (Fei Ye)

Academic Editor: Amancio Carnero Moya
Submitted: 22 November 2025 Revised: 25 January 2026 Accepted: 29 January 2026 Published: 13 February 2026

Abstract

Background: Malignant gliomas remain largely refractory to current therapies, in part because abnormal tumor vasculature and a disrupted blood-brain barrier limit intratumoral drug delivery and cause severe tumor-associated edema. The oncolytic adenovirus KD01 is a conditionally replicating adenovirus type 5 with a 27-bp deletion in Early Region 1A (E1A) and a truncated BH3-Interacting Domain Death Agonist (tBID) expression cassette inserted into the E3 region. This study investigated whether bevacizumab-induced vascular normalization would enhance the delivery and efficacy of KD01 in gliomas. **Methods**: The oncolytic activity and mitochondrial effects of KD01 were evaluated in human glioma cell lines using cell viability assays, JC-1 staining, quantitative real-time-polymerase chain reaction (qRT-PCR), and western blotting for BID/tBID. An orthotopic LN229 nude mouse model was used to assess a sequential bevacizumab→KD01 regimen. Mice were randomized to receive PBS, bevacizumab, KD01, or combination treatment. Body weight and survival were recorded. Tumor cell proliferation (Ki-67), tumor vasculature (CD31), brain water content (ΔWater%), serum biochemistry, coagulation parameters, and organ weights were analyzed to evaluate antitumor activity, edema, and systemic safety. **Results**: KD01 induced robust dose- and time-dependent cytotoxicity in glioma cells and caused marked mitochondrial depolarization, accompanied by increased BID mRNA expression, loss of full-length BID, and accumulation of tBID. In the orthotopic LN229 model, bevacizumab administered 48 h before KD01 significantly improved overall outcomes compared with either monotherapy. The bevacizumab→KD01 group showed improved preservation of body weight, pronounced prolongation of survival, and the lowest Ki-67 labeling index. This group also exhibited reduced brain water content (ΔWater%), consistent with sparser CD31-positive vessels resulting from vascular normalization and oncolysis, indicating effective attenuation of tumor-associated edema. Serum liver and kidney function tests, platelet counts, coagulation indices, and major organ weights were comparable across treatment groups, suggesting no additional systemic toxicity associated with combination treatment. **Conclusions**: KD01 exerts potent tBID-mediated mitochondrial oncolytic activity against glioma cells. When used as a priming strategy, transient vascular normalization induced by bevacizumab enhanced the intratumoral efficacy of KD01 in an orthotopic glioma model while maintaining a favorable safety profile. These findings support a simple, sequence-dependent combination approach integrating anti-VEGF therapy with oncolytic virotherapy for the treatment of malignant gliomas.

Keywords: glioma; adenovirus; oncolytic virotherapy; KD01; bevacizumab; vascular normalization

1. Introduction

Malignant gliomas, particularly glioblastomas, are among the most aggressive primary brain tumors in adults [1]. Even with current standard-of-care regimens combining maximal safe resection with radiotherapy and temozolomide, median overall survival rarely exceeds 15–20 months [1]. Treatment failure reflects not only marked genetic and phenotypic heterogeneity but also profoundly abnormal tumor vasculature and disruption of the blood-brain barrier. These vascular abnormalities severely restrict intratumoral drug delivery and distribution and contribute to pronounced tumor-associated brain edema [2]. Together, these features highlight the need for therapeutic strategies that can efficiently kill tumor cells while overcoming vascular barriers within the brain.

Bevacizumab, a recombinant humanized monoclonal antibody targeting vascular endothelial growth factor (VEGF), has been incorporated into glioblastoma management as an antiangiogenic agent [3]. Clinical trials have shown that bevacizumab can rapidly reduce contrast enhancement and peritumoral edema and improve progression-free survival; however, its impact on overall survival is modest, and resistance is nearly universal [4]. The concept of "vascular normalization" provides a plausible explanation for these paradoxical findings. Short-term, appropriately dosed VEGF blockade can transiently remodel chaotic, leaky tumor vessels into a more structurally organized and homogeneously perfused network, thereby improving drug penetration during a limited time window [5]. However, in malignant glioma, it remains unclear how best to exploit this normalization window, par-

ticularly in combination with biological agents such as oncolytic viruses, and how treatment sequence and timing influence therapeutic efficacy.

Oncolytic virotherapy offers a complementary approach for malignant gliomas by combining selective tumor cell lysis with the potential to activate antitumor immune responses [6]. Among available platforms, adenovirus type 5–based vectors are particularly attractive because of their well-characterized biology and amenability to genetic engineering [7]. KD01 is a recombinant oncolytic adenovirus derived from adenovirus type 5, engineered with a 27-bp deletion in a conserved region of Early Region 1A (E1A) to confer preferential replication in tumor cells. In addition, the E3 region is modified by deletion of the adenovirus death protein (ADP) and insertion of a truncated BH3-Interacting Domain Death Agonist (tBID) expression cassette [8]. tBID is a potent proapoptotic molecule that translocates to mitochondria and promotes mitochondrial outer membrane permeabilization, thereby amplifying intrinsic apoptotic signaling [9]. Previous studies in non–central nervous system tumor models have shown that KD01 and related tBID-armed vectors induce strong oncolytic effects, mitochondrial apoptosis, and immunogenic cell death with favorable safety profiles. However, their activity in gliomas and interactions with abnormal cerebral vasculature have not been systematically characterized [10].

Based on these considerations, we hypothesized that transient vascular normalization induced by bevacizumab could enhance intratumoral delivery and antitumor efficacy of KD01 in gliomas. Specifically, we postulated that administering bevacizumab within an appropriate time window before local KD01 injection would reduce vascular leakiness and tumor-associated brain edema, improve perfusion and viral distribution, and thereby potentiate tBID-mediated tumor cell killing without increasing systemic toxicity. To test this hypothesis, we evaluated the oncolytic activity of KD01 and its effects on mitochondrial function in human glioma cell lines *in vitro*. We further used an orthotopic LN229 nude mouse model to systematically assess the effects of a sequential bevacizumab–KD01 regimen on survival, tumor cell proliferation, brain water content, and systemic safety. By combining a tBID-armed oncolytic adenovirus with a clinically available anti-VEGF therapy, we aimed to provide preclinical evidence for a simple, sequence-dependent combination strategy to improve oncolytic virotherapy for malignant gliomas.

2. Materials and Methods

2.1 Cell Lines and Culture

Human glioma cell lines A172 and LN229 were obtained from the Cell Bank of the Chinese Academy of Sciences (Shanghai, China) and authenticated by short tandem repeat profiling within 6 months before use. Cells were cultured in Dulbecco's modified Eagle's medium (DMEM; Gibco, Thermo Fisher Scientific, Grand Island, NY, USA, catalog number 11965092) supplemented with 10% fetal bovine serum (FBS; Gibco, 16140071, Grand Island, NY, USA), 100 U/mL penicillin, and 100 µg/mL streptomycin at 37 °C in a humidified incubator with 5% CO_2. Cells were routinely tested and confirmed to be mycoplasma-free.

2.2 Oncolytic Adenovirus KD01 and Control Virus

KD01 is a recombinant oncolytic adenovirus type 5 carrying a 27-bp deletion in the conserved E1A region and an engineered E3 region in which ADP is deleted and replaced by a tBID expression cassette. A replication-competent adenovirus with an ADP deletion but without tBID insertion (M20) was used as the control virus. Viral stocks were propagated in HEK293 cells, purified by double cesium chloride gradient ultracentrifugation, and dialyzed against storage buffer (10 mM Tris–HCl, 2 mM $MgCl_2$, 5% glycerol, pH 8.0). Viral particle (vp) concentrations were determined spectrophotometrically at 260 nm, and infectious titers PFU (Plaque-Forming Units) were determined using plaque assays in HEK293 cells. Viruses were stored at –80 °C until use.

2.3 Cell Viability Assay

To assess oncolytic activity *in vitro*, A172 and LN229 cells were seeded into 96-well plates at a density of 5×10^3 cells per well and allowed to adhere overnight. Cells were infected with KD01 at the indicated multiplicities of infection (MOIs; 0.1, 1, and 10) in serum-free medium for 2 h, after which the medium was replaced with complete growth medium. Cell viability was measured at 24, 48, and 72 h post-infection using a Cell Counting Kit-8 (CCK-8; Beyotime Biotechnology, Shanghai, China, catalog number C0037), according to the manufacturer's instructions. Absorbance was measured at 450 nm using a microplate reader (BioTek Instruments, Inc., Winooski, VT, USA), and cell viability was expressed as a percentage of the mock-treated control.

2.4 Mitochondrial Membrane Potential Assay

Mitochondrial membrane potential ($\Delta\psi$m) was assessed using a JC-1 assay kit (Beyotime Biotechnology, Shanghai, China, catalog number C2006). LN229 cells were seeded into 24-well plates, infected with PBS, M20, or KD01 (MOI = 1), and incubated for 24 h. Cells were then incubated with JC-1 working solution at 37 °C for 20 min, washed with JC-1 buffer, and imaged using a fluorescence microscope (Leica Microsystems, Wetzlar, Germany). Red fluorescence (JC-1 aggregates) and green fluorescence (JC-1 monomers) were recorded. The ratio of red to green fluorescence intensity was quantified using ImageJ (version 1.53t; National Institutes of Health, Bethesda, MD, USA) and used as an index of $\Delta\psi$m.

2.5 Quantitative Real-time PCR

Total RNA was extracted from LN229 cells using TRIzol reagent (Invitrogen, Thermo Fisher Scientific, Carlsbad, CA, USA), and 1 µg of RNA was reverse-transcribed using a PrimeScript RT kit (Takara Bio Inc., Kusatsu, Shiga, Japan, catalog number RR037A). Quantitative real-time PCR (qRT-PCR) was performed using TB Green Premix (Takara) on a QuantStudio 6 System (Applied Biosystems, Thermo Fisher Scientific, Carlsbad, CA, USA). Primers for human BID and GAPDH (internal control) were designed using Primer-BLAST. Relative BID mRNA expression was calculated using the $2^{-\Delta\Delta Ct}$ method. The detailed gene sequences are listed in Table 1.

Table 1. Primer sequences for qRT-PCR detection of BID and GAPDH genes.

Gene	Primer type	Primer sequence
BID	Forward	5′-CCAGGCTGTTTGAGGACCTC-3′
	Reverse	5′-TGTGGGCTGCTTGTCTCTG-3′
GAPDH	Forward	5′-GGAGCGAGATCCCTCCAAAAT-3′
	Reverse	5′-GGCTGTTGTCATACTTCTCATGG-3′

qRT-PCR, Quantitative real-time PCR; BID, BH3-interacting domain death agonist; GAPDH, Glyceraldehyde-3-phosphate dehydrogenase.

2.6 Western Blot Analysis

Protein expression of BID and tBID was examined by western blotting. LN229 cells were infected with KD01 at different MOIs (0, 1, and 10) for 24 h and lysed in RIPA buffer supplemented with protease inhibitors (Beyotime). Equal amounts of protein were separated by SDS-polyacrylamide gel electrophoresis and transferred onto PVDF membranes (Merck Millipore, Burlington, MA, USA). Membranes were blocked with 5% nonfat milk and incubated overnight at 4 °C with primary antibodies against BID (ABclonal Technology, Wuhan, China, catalog number A23234) and β-actin (ABclonal Technology, Wuhan, China, catalog number AC028), followed by incubation with horseradish peroxidase-conjugated secondary antibodies. Protein bands were visualized using enhanced chemiluminescence (ECL; Millipore, Burlington, MA, USA) and quantified using ImageJ software.

2.7 Orthotopic Glioma Model and Treatment

All animal procedures were approved by the Animal Experimentation Ethics Committee of Tongji Medical College (protocol code 4704) and were conducted in accordance with institutional guidelines.

Male BALB/c nude mice (4–6 weeks old; Jicui Biotechnology, Guangdong, China) were anesthetized with isoflurane and positioned in a stereotactic frame. LN229 cells (1×10^7 cells in 5 µL PBS) were injected into the right striatum (2.0 mm lateral and 1.0 mm anterior to bregma, at a depth of 3.0 mm) at a rate of 0.5 µL/min using a Hamilton syringe. The needle was left in place for 5 min before slow withdrawal to prevent reflux.

Tumor-bearing mice were randomly assigned to four groups (n = 11 per group): PBS control, bevacizumab alone, KD01 alone, and bevacizumab followed by KD01 (Bev→KD01). Bevacizumab (Roche, Basel, Switzerland) was administered intraperitoneally at 10 mg/kg on day 7 after tumor implantation. KD01 was administered via stereotactic intratumoral injection at a dose of 1×10^9 viral particles (vp) in 5 µL PBS on day 9. Mice in the KD01-alone group received KD01 on day 9 without bevacizumab, those in the bevacizumab-alone group received bevacizumab on day 7 without KD01, and control mice received equal volumes of PBS. Body weight and clinical signs were monitored twice weekly; and survival was recorded from the day of tumor implantation until the humane endpoint was reached.

At the experimental endpoint, mice were humanely euthanized by intraperitoneal (i.p.) injection of an overdose of sodium pentobarbital (200 mg/kg body weight). This method induces rapid, painless anesthesia, followed by the cessation of vital functions, ensuring minimal distress to the animals. Successful euthanasia was confirmed by the absence of corneal reflexes and respiratory and cardiac activity.

2.8 Brain Water Content

Tumor-associated brain edema was assessed by measuring brain water content. On Day 5 after KD01 treatment (day 14 after tumor implantation), three mice from each group were randomly selected and subjected to deep anesthesia followed by decapitation. The brain was rapidly removed, and the tumor-bearing and contralateral hemispheres were dissected and weighed to obtain wet weights. Samples were then dried at 100 °C for 24 h and reweighed to obtain dry weights. Brain water content (%) was calculated as:

Water content = (wet weight – dry weight)/wet weight $\times$ 100%

The difference in water content between the tumor-bearing and contralateral hemispheres (ΔWater%) was used as an index of tumor-associated edema.

2.9 Immunohistochemistry

For Ki-67 and CD31 staining, mice were transcardially perfused with PBS, followed by 4% paraformaldehyde. Brains were harvested, fixed overnight, paraffin-embedded, and sectioned at 4 µm. Sections were deparaffinized, rehydrated, subjected to antigen retrieval (citrate buffer, pH 6.0), and blocked with 5% bovine serum albumin. Sections were incubated overnight at 4 °C with primary antibodies against Ki-67 (Abcam, Waltham, MA, USA, catalog number ab15580) or CD31 (Abcam), fol-

lowed by incubation with HRP-conjugated secondary antibodies. Immunoreactivity was visualized with DAB substrate and counterstained with hematoxylin. The Ki-67 labeling index was calculated as the percentage of Ki-67-positive nuclei counted in $\geq$5 random high-power fields per tumor. CD31 staining was evaluated to assess vascular distribution in the same tissue sections.

2.10 Serum Biochemistry, Coagulation and Organ Weights

To evaluate systemic toxicity, blood samples were collected from the retro-orbital sinus at the experimental endpoint. Serum levels of alanine aminotransferase (ALT), aspartate aminotransferase (AST), alkaline phosphatase (ALP), and creatinine (CREA) were measured using an automated biochemical analyzer (Cobas 8000 Modular Analyzer; Roche Diagnostics, Switzerland). Platelet counts (PLT) and prothrombin time (PT) were measured using hematology and coagulation analyzers, respectively. Major organs, including the brain, liver, and spleen, were excised and weighed.

2.11 Statistical Analysis

Data are presented as mean $\pm$ standard error of the mean (SEM) unless otherwise stated. Comparisons between two groups were performed using unpaired two-tailed Student's *t*-tests. Comparisons among multiple groups were performed using one-way analysis of variance (ANOVA) followed by Tukey's post hoc test. Survival curves were generated using the Kaplan–Meier method and compared using the log-rank (Mantel–Cox) test. Statistical significance was defined as $p < 0.05$. All statistical analyses were performed using GraphPad Prism 10 (version 10.0.3; GraphPad Software, San Diego, CA, USA).

3. Results

3.1 KD01 Design and Oncolytic Activity in Human Glioma Cells

To generate a conditionally replicating oncolytic adenovirus, KD01 was engineered with a small deletion in the conserved region of E1A (Δ920–926 bp) and with replacement of ADP in the E3 region by a tBID expression cassette (Fig. 1A).

We first examined the intrinsic susceptibility of human glioma cells to KD01. Infection of LN229 cells with increasing MOIs of KD01 (0.1, 1, and 10) resulted in a clear dose- and time-dependent reduction in cell viability (Fig. 1B). Even at an MOI of 0.1, KD01 significantly reduced cell viability compared with controls at 48 and 72 h. At an MOI of 10, viability decreased to a small fraction of control levels by 72 h ($p < 0.01$). A similar pattern was observed in A172 cells (Fig. 1C), with significant loss of viability at MOIs $\geq$0.1 over time, although the extent of cytotoxicity was slightly less pronounced than in LN229 cells at equivalent doses. Collectively, these results indicate that KD01 exerts potent dose- and time-dependent oncolytic activity against human glioma cell lines *in vitro*.

3.2 KD01 Triggers tBID-mediated Mitochondrial Dysfunction in Glioma Cells

To investigate whether KD01 exerts cytotoxicity through mitochondrial apoptosis, we first assessed mitochondrial membrane potential using JC-1 staining. In LN229 cells treated with PBS, strong red JC-1 aggregates and weak green fluorescence were observed, indicating an intact mitochondrial membrane potential (Fig. 2A). Infection with the control virus M20 caused a moderate increase in green fluorescence and a reduction in red aggregates, whereas KD01 infection led to a marked loss of red fluorescence with predominantly green staining, consistent with mitochondrial depolarization. Quantification of the JC-1 aggregate/monomer ratio confirmed that KD01 induced significantly greater disruption of the mitochondrial membrane potential than M20 (Fig. 2B).

Given that KD01 encodes tBID, we next examined BID/tBID expression. KD01 infection increased BID transcript levels in a dose-dependent manner (Fig. 2C). At the protein level, full-length BID was progressively reduced, whereas tBID accumulated with increasing MOIs of KD01 (Fig. 2D,E), indicating efficient expression and processing of the tBID cassette. Taken together, these data demonstrate that KD01 potently activates the BID–tBID pathway and induces profound mitochondrial dysfunction in glioma cells, consistent with engagement of the intrinsic apoptotic pathway.

3.3 Bevacizumab Priming Significantly Enhances the Antitumor Efficacy of KD01 in the LN229 Orthotopic Glioma Model

As shown in Fig. 3A, we evaluated the effects of bevacizumab combined with KD01 using a sequential treatment schedule in a nude mouse LN229 intracranial xenograft model. On day 0 (D0), LN229 cells were inoculated into the brain by stereotactic injection; on day 7 (D7), mice received an intraperitoneal injection of bevacizumab or PBS; and on day 9 (D9), KD01 or PBS was administered via stereotactic intratumoral injection. This design generated four treatment groups: PBS, KD01, bevacizumab, and KD01 + bevacizumab, and animals were monitored until death.

Body weight changes were compared among groups as an indirect measure of systemic toxicity and overall condition. Throughout the observation period, mice in the PBS and KD01 groups showed a gradual decline in body weight, whereas body weight in the bevacizumab group remained largely stable. Notably, in the combination group, body weight did not decrease and was consistently higher than that in the PBS and KD01 groups from D10 onward (Fig. 3B). On D14, D21, and D28, body weight in the KD01 + bevacizumab group was significantly higher than that in the KD01 monotherapy group ($p < 0.05$), indicating that, at the doses used, the combination regimen did not increase systemic toxicity and was associated with better clinical status than KD01 alone.

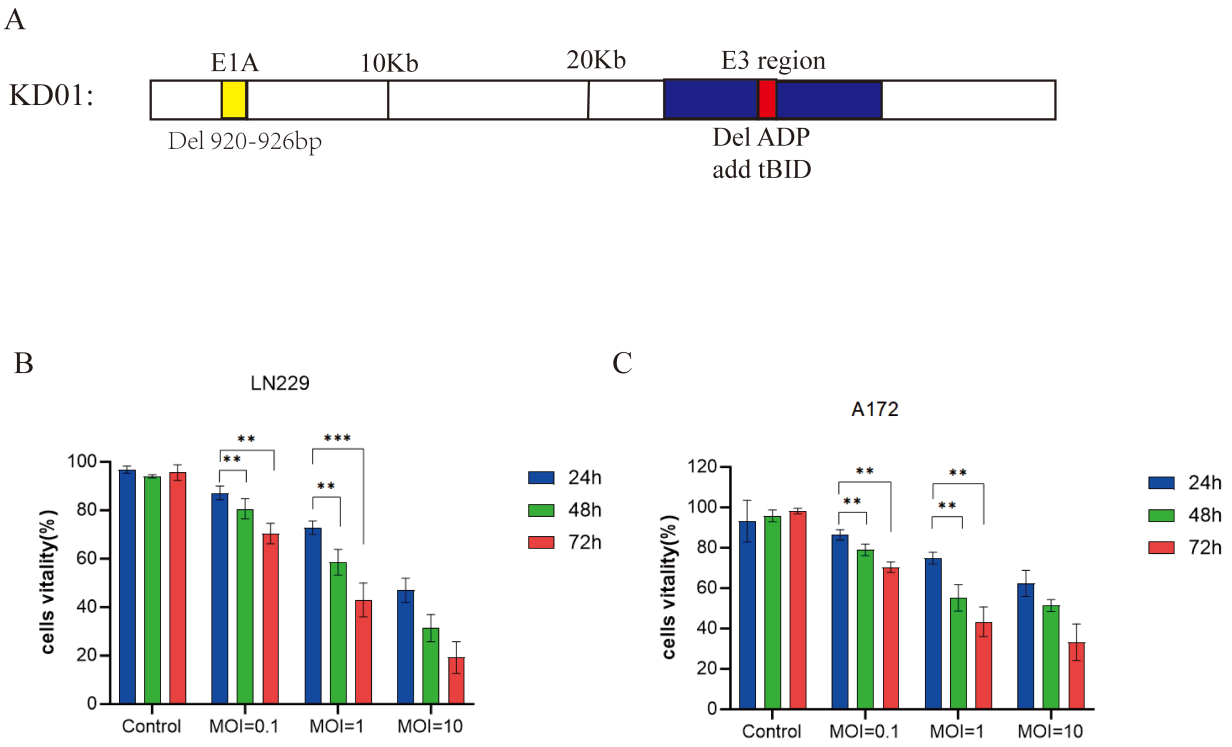

Fig. 1. Structure of KD01 and its oncolytic activity in human glioma cells. (A) Schematic representation of KD01. A 27-bp deletion was introduced into the conserved region of E1A (Δ920–926 bp), and the ADP in the E3 region was deleted and replaced by a tBID expression cassette. (B,C) Cell viability of human glioma cell lines LN229 (B) and A172 (C) after infection with KD01 at the indicated multiplicities of infection (MOI 0.1, 1, and 10) or mock infection (Control). Cell viability was measured using the CCK-8 assay at 24, 48 and 72 h post-infection and expressed as a percentage of the corresponding control. Data are presented as mean ± SEM (n = [6]); statistical significance between the indicated groups is shown as $^{**}p < 0.01$ and $^{***}p < 0.001$. ADP, adenovirus death protein; tBID, truncated BID; MOI, multiplicities of infection; CCK-8, Cell Counting Kit-8.

Kaplan–Meier survival analysis further confirmed that KD01 combined with bevacizumab significantly prolonged survival in tumor-bearing mice (Fig. 3C). Animals in the PBS group developed neurological deterioration shortly after implantation and died sequentially. Bevacizumab or KD01 monotherapy delayed death to some extent, but survival curves declined rapidly. In contrast, the survival curve of the KD01 + bevacizumab group shifted markedly to the right, with most mice surviving longer than those in the three control groups. Log-rank testing revealed statistically significant differences between the combination group and the KD01, bevacizumab, and PBS groups, indicating that sequential bevacizumab priming markedly enhanced the *in vivo* antitumor efficacy of KD01.

Tumor cell proliferation was next assessed using Ki-67 immunohistochemistry. In the PBS group, strong brown nuclear Ki-67 staining was diffusely distributed throughout the tumor, resulting in the highest Ki-67 labeling index. The proportion of Ki-67–positive cells was clearly reduced in both the KD01 and bevacizumab groups, although numerous positive cells remained. In the KD01 + bevacizumab group, Ki-67–positive cells were markedly decreased, with only scattered weakly positive nuclei and much lower overall staining intensity. Semi-quantitative analysis showed that the Ki-67 labeling index was lowest in the combination group and was significantly lower than that in the PBS and monotherapy groups (Fig. 3D).

To evaluate the effect of combination therapy on tumor-associated brain edema, we measured the difference in water content between the tumor-bearing and contralateral hemispheres (ΔWater%). Quantitative analysis revealed that ΔWater% was highest in the PBS group, slightly reduced in the KD01 and bevacizumab groups, and significantly lower in the KD01 + bevacizumab group compared with all three control groups ($p < 0.05$, Fig. 3E). These findings indicate that bevacizumab priming not only enhances the survival benefit of KD01 but also cooperatively alleviates tumor-associated brain edema, likely contributing to the improved overall condition of treated animals.

Tumor vascular density was evaluated using CD31 (an endothelial cell marker) staining (Fig. 3F,G). The PBS group exhibited dense, disorganized CD31-positive vessels. KD01 monotherapy mildly reduced vascular density, whereas bevacizumab alone induced a more pronounced

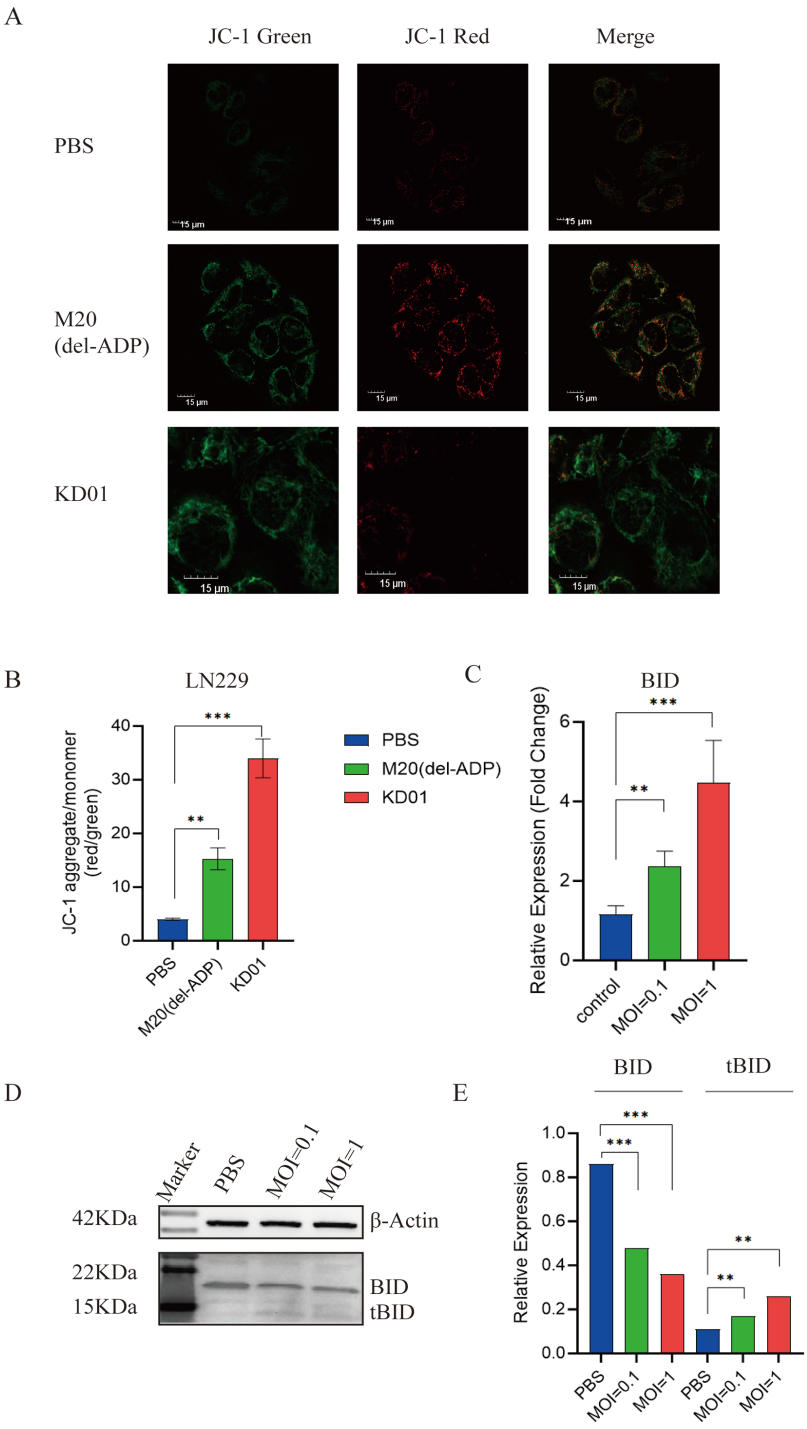

Fig. 2. KD01 induces mitochondrial dysfunction via activation of the BID–tBID pathway in glioma cells. (A) Representative JC-1 staining of LN229 cells treated with PBS, control virus M20 (Del-ADP), or KD01. Red fluorescence indicates JC-1 aggregates in mitochondria with intact membrane potential, and green fluorescence indicates JC-1 monomers in depolarized mitochondria (scale bar, 15 μm). (B) Quantification of mitochondrial membrane potential expressed as the ratio of JC-1 aggregates to monomers (red/green) in LN229 cells after the indicated treatments. (C) Relative BID mRNA expression in LN229 cells infected with KD01 at MOI 0.1 or 1 compared with PBS control, determined by qRT-PCR. (D) Representative Western blot of full-length BID and tBID protein in LN229 cells infected with KD01 at the indicated MOIs; β-actin served as a loading control. (E) Densitometric analysis of BID and tBID protein levels normalized to β-actin. Data in (B), (C), and (E) are presented as mean ± SEM (n = 3 independent experiments). $^{**}p < 0.01$, $^{***}p < 0.001$.

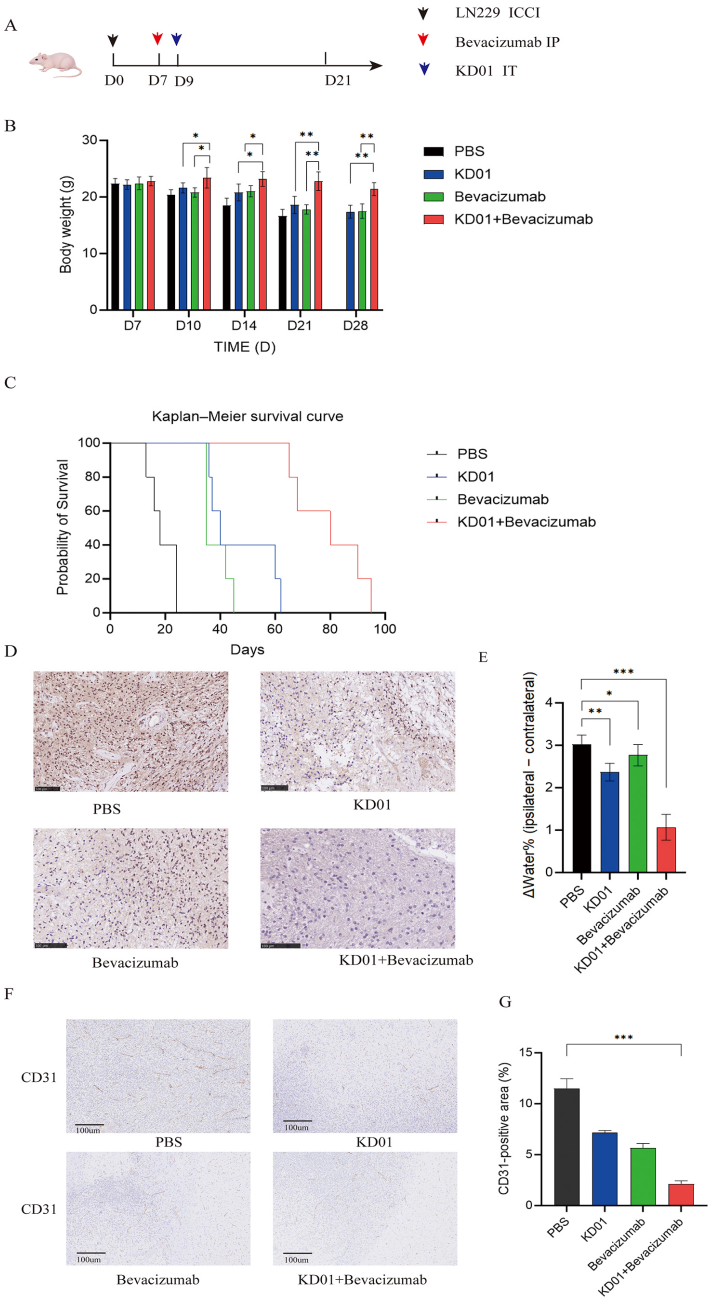

Fig. 3. Bevacizumab priming enhances antitumor efficacy of KD01 in an orthotopic LN229 glioma model. (A) Schematic of the treatment schedule. LN229 cells were implanted intracranially on day 0 (D0). Mice received intraperitoneal bevacizumab or PBS on day 7 (D7) and stereotactic intratumoral injection of KD01 or PBS on day 9 (D9), generating four groups: PBS, KD01, bevacizumab, and KD01 + bevacizumab. (B) Body weight changes in each group at the indicated time points. Data are shown as mean ± SEM (n = [5]); the combination group maintained significantly higher body weight than the KD01 group at D14, D21, and D28. (C) Kaplan–Meier survival curves for tumor-bearing mice in the four treatment groups. Sequential bevacizumab + KD01 treatment markedly prolonged survival compared with PBS, KD01, or bevacizumab alone (log-rank test). (D) Representative Ki-67 immunohistochemistry of intracranial tumors from each group (scale bar, 100 μm). Strong, diffuse nuclear Ki-67 staining is seen in the PBS group, reduced staining in the KD01 and bevacizumab groups, and the weakest staining in the KD01 + bevacizumab group. (E) Tumor-associated brain edema assessed as the difference in water content between tumor-bearing and contralateral hemispheres (ΔWater%). ΔWater% was highest in the PBS group, slightly reduced in the KD01 and bevacizumab groups, and significantly lowest in the KD01 + bevacizumab group. (F) CD31 immunohistochemical staining of tumor vasculature in each treatment group (scale bar, 100 μm). (G) Statistical analysis of CD31-positive area percentage (n = 5). Data are presented as mean ± SEM (n = [3]); ICCI, Intracranial Injection; IP, Intraperitoneal Injection; IT, Intratumoral Injection. *$p < 0.05$, **$p < 0.01$, ***$p < 0.001$.

decrease. Notably, the KD01 + bevacizumab combination group displayed the sparsest CD31 staining, with only scattered vascular structures, consistent with synergistic vascular remodeling by bevacizumab-mediated normalization and KD01-induced oncolytic disruption.

3.4 KD01 Combined With Bevacizumab Does Not Induce Obvious Systemic Toxicity

To further evaluate systemic safety of sequential KD01 and bevacizumab treatment, serum biochemical and coagulation parameters were measured at the study endpoint, and major organ weights were compared among groups. Serum AST, ALP, and CREA levels remained within physiological ranges in all groups, with no statistically significant differences between the KD01, bevacizumab, or KD01 + bevacizumab groups and the PBS control group (Fig. 4A–C). ALT levels were slightly higher in the KD01 and bevacizumab monotherapy groups than in the PBS group; however, the increase was modest, and ALT levels in the KD01 + bevacizumab group were comparable to PBS (Fig. 4D). These findings suggest that either virus or anti-VEGF monotherapy may cause mild, tolerable fluctuations in liver function that are not exacerbated by the combination regimen.

PLT and PT values were also similar across all four groups (Fig. 4E,F), indicating that neither KD01 nor bevacizumab, alone or in combination, significantly affected coagulation function or platelet production. Likewise, relative weights of major organs, including the brain, spleen, and liver, did not differ significantly among the PBS, KD01, bevacizumab, and KD01 + bevacizumab groups (Fig. 4G), and no obvious organ atrophy or enlargement was observed.

Taken together, these results indicate that sequential bevacizumab priming combined with KD01 oncolytic therapy did not induce hepatic or renal injury, coagulation abnormalities, or major organ toxicity at the doses and schedules used in this study, supporting a favorable systemic safety profile for this combination strategy.

4. Discussion

In this study, we systematically investigated the application of the tBID-armed, conditionally replicating adenovirus KD01 in gliomas and evaluated the feasibility of its sequential combination with bevacizumab. We demonstrated that KD01 exerts robust, dose- and time-dependent oncolytic activity against the human glioma cell lines LN229 and A172, indicating that glioma cells with distinct molecular backgrounds are highly susceptible to this vector. Mechanistically, KD01 infection led to a marked loss of mitochondrial membrane potential, accompanied by a decrease in full-length BID and pronounced accumulation of tBID, indicating activation of the BID–tBID axis and engagement of the intrinsic mitochondrial apoptotic pathway. These findings not only confirm effective expression and functional activity of tBID within the KD01 backbone but also provide a molecular basis for the strong oncolytic effects of this virus.

We therefore focused on the *in vivo* effects of combining anti-VEGF therapy with KD01. Compared with either KD01 or bevacizumab alone, sequential bevacizumab plus KD01 treatment produced a more pronounced survival benefit in an orthotopic LN229 nude mouse model. Mice in the combination group exhibited a smaller decline in body weight, and Kaplan–Meier analysis revealed a significant prolongation of median survival, indicating that bevacizumab priming can markedly enhance the overall therapeutic efficacy of KD01. At the histopathological level, Ki-67 staining was weakest in the combination group, with the lowest proportion of Ki-67–positive tumor cells among all treatment arms, further supporting the superior antiproliferative effect of the combination regimen.

A major cause of treatment failure in gliomas is the combination of severely disorganized tumor vasculature and blood-brain barrier disruption, which results in poor drug delivery and pronounced cerebral edema [11,12]. Previous clinical trials have shown that bevacizumab can rapidly reduce radiographic enhancement and brain edema; however, its impact on overall survival remains limited, suggesting that VEGF blockade alone is insufficient to fundamentally alter disease progression [13]. The vascular normalization hypothesis proposes that short-term, moderate inhibition of VEGF can remodel abnormal tumor vessels into a more orderly and less permeable network, thereby improving perfusion and drug delivery [14]. In the present study, sequential administration of bevacizumab and KD01 significantly reduced water content in the tumor-bearing hemisphere, with marked alleviation of peritumoral interstitial edema and exudation. These changes were consistent with improvements in body weight and survival and indirectly support the existence of a bevacizumab-induced "vascular normalization window" that is conducive to viral delivery in this model [15]. Administration of KD01 within this window likely allows more uniform and deeper viral penetration into the tumor core and infiltrative margins, thereby amplifying its oncolytic and pro-apoptotic effects.

Importantly, the enhanced antitumor activity achieved with the combination regimen was not accompanied by increased systemic toxicity. Serum biomarkers of liver and kidney function (AST, ALT, ALP, CREA) did not differ significantly among groups, and coagulation parameters and platelet counts were unaffected. Consistent with these findings, no obvious changes were observed in the weights of major organs, including the brain, spleen, and liver. Together, these results suggest that, at the doses and schedules used in this study, bevacizumab priming does not exacerbate the systemic toxicity of KD01, supporting further development of this combination strategy from a safety perspective.

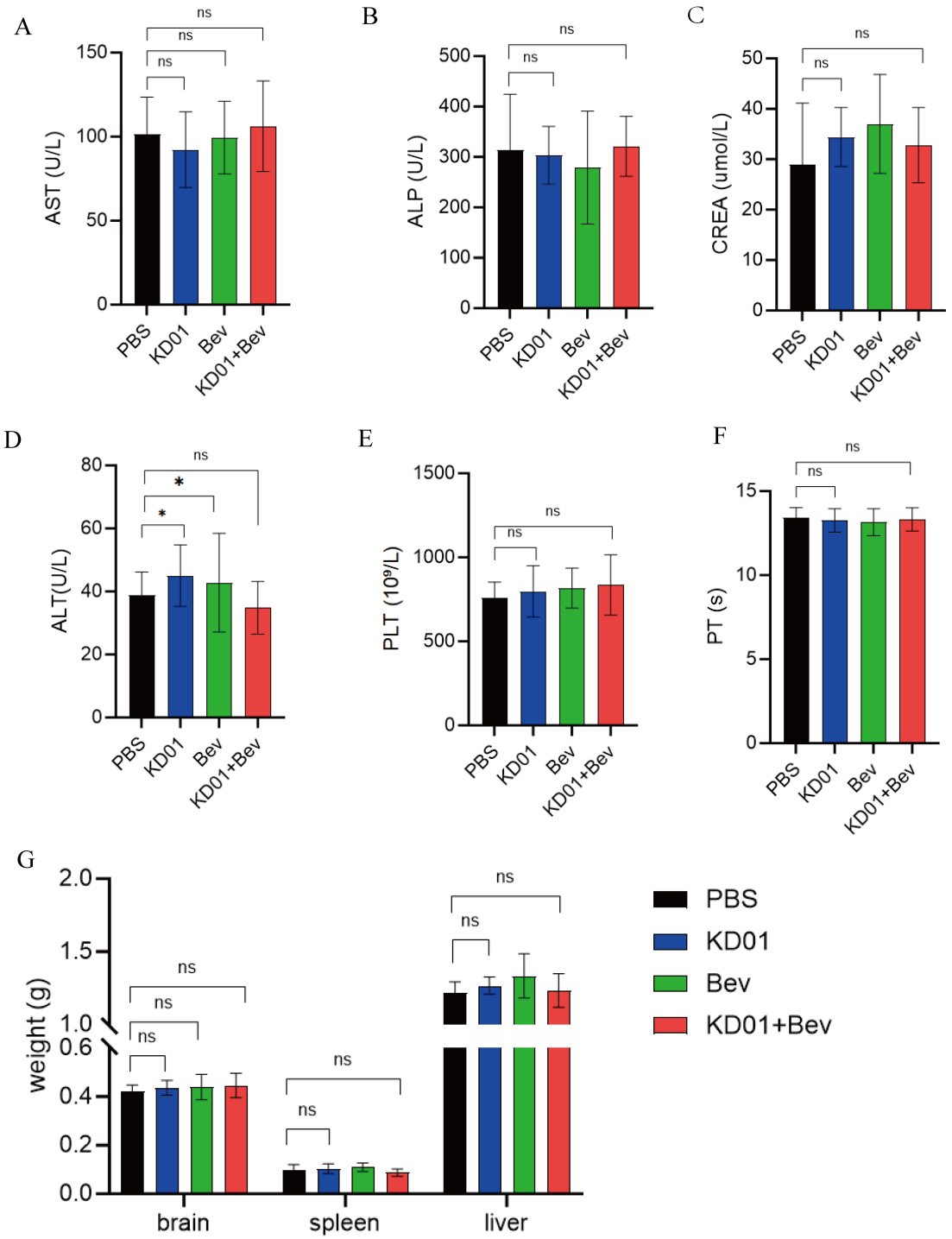

Fig. 4. Systemic safety of sequential KD01 and bevacizumab treatment in tumor-bearing mice. (A–D) Serum biochemical parameters at the end of the study: AST (A), ALP (B), CREA (C), and ALT (D) in mice treated with PBS, KD01, Bev, or KD01 + Bev. AST, ALP, and CREA remained within the physiological range with no significant intergroup differences; ALT showed a mild increase in the KD01 and Bev monotherapy groups but returned to control levels in the combination group. (E,F) PLT (E), and PT (F) among the four groups, showing no significant effects of KD01, Bev, or their combination on coagulation function or platelet production. (G) Relative weights of major organs (brain, spleen, and liver) at sacrifice. No significant differences were observed among groups, and no obvious organ atrophy or enlargement was detected. Data are presented as mean ± SEM (n = [3]). Bev, bevacizumab; AST, aspartate aminotransferase; ALP, alkaline phosphatase; CREA, creatinine; ALT, alanine aminotransferase; PLT, Platelet counts; PT, prothrombin time. *$p < 0.05$; ns, not significant.

Our findings are also consistent with accumulating evidence supporting the combination of oncolytic viruses with antiangiogenic or immune-based therapies [16]. Previous studies have shown that appropriately tuned vascular normalization can facilitate intratumoral viral spread and enhance immune cell infiltration into the tumor microenvironment [17]. KD01 is characterized by tumor-selective replication, potent activation of mitochondrial apoptosis, and the potential induction of immunogenic cell death through tBID expression. In principle, this mode of tumor cell death, together with improved perfusion and reduced interstitial pressure during vascular normalization, may elicit a stronger antitumor immune response [18]. Although immune cell infiltration and functional antitumor immunity were not directly assessed in this study, these potential synergistic mechanisms warrant further investigation in immunocompetent models.

Some limitations of this study should be acknowledged. First, the *in vivo* efficacy of KD01 and bevacizumab was evaluated using a single human glioma cell line–derived orthotopic nude mouse model. Validation in additional models, including patient-derived organoids and glioma stem-like cells, is necessary to improve the generalizability of these findings [19]. Second, assessment of vascular normalization and edema was based primarily on brain water content measurements and conventional histology. Advanced imaging modalities, such as dynamic contrast-enhanced MRI, perfusion imaging, or spatiotemporal mapping of viral distribution, were not employed. Consequently, the precise onset and duration of the vascular normalization window could not be defined or quantitatively linked to viral delivery [20]. Third, the doses and timing of bevacizumab and KD01 administration were empirically selected rather than systematically optimized. Future dose–response and schedule–optimization studies may further enhance therapeutic efficacy or permit dose reductions [21]. Finally, immune effects are an integral component of oncolytic virotherapy [22]; however, our *in vivo* experiments were conducted predominantly in immunodeficient mice, limiting our ability to fully capture the impact of KD01 and bevacizumab on the tumor immune microenvironment. Addressing these issues is important in future studies.

It is also important to consider potential clinical challenges that may limit the translational applicability of this regimen. Pre-existing neutralizing antibodies (NAbs) against adenovirus type 5 are highly prevalent in human populations and could substantially reduce intratumoral delivery and replication of KD01 by sequestering viral particles before they reach glioma tissue. Strategies such as capsid engineering or transient immunosuppression may be required to mitigate this effect. Additionally, although bevacizumab can normalize tumor vasculature in preclinical models, its penetration across the intact blood-brain barrier in human gliomas is limited, particularly in infiltrative tumor regions with relatively preserved barrier integrity. This limitation may restrict the induction of a functional vascular normalization window in clinically relevant compartments, necessitating adjunctive approaches, such as blood-brain barrier-disrupting techniques or convection-enhanced delivery, to improve bevacizumab distribution within the brain. These challenges highlight the need for tailored strategies to bridge preclinical efficacy and clinical application.

In summary, this study demonstrates that the tBID-armed, conditionally replicating adenovirus KD01 exerts potent oncolytic activity against glioma cells *in vitro* and *in vivo*, and that bevacizumab-induced vascular normalization can significantly enhance its antitumor efficacy in an orthotopic glioma model while reducing brain edema without increasing systemic toxicity. These findings provide experimental support for a sequential "anti-VEGF priming plus oncolytic adenovirus" strategy for malignant glioma. This approach merits further evaluation in advanced preclinical models and early-phase clinical trials, including its integration with radiochemotherapy and immune checkpoint blockade as part of multimodal glioma treatment.

5. Conclusion

In conclusion, this study demonstrates that the tBID-armed, conditionally replicating adenovirus KD01 exerts potent mitochondria-dependent oncolytic activity against human glioma cells. In an orthotopic LN229 model, transient bevacizumab priming significantly enhanced the therapeutic efficacy of KD01, as evidenced by improved body weight maintenance, prolonged survival, reduced Ki-67 proliferation, and attenuation of tumor-associated brain edema, without introducing appreciable systemic toxicity. These findings support a simple, sequence-dependent combination strategy in which anti-VEGF-mediated vascular normalization is exploited to improve intratumoral delivery and antitumor activity of oncolytic adenoviruses in malignant gliomas. Further preclinical and early-phase clinical studies are warranted to optimize dosing and timing and to explore integration of this approach into multimodal treatment regimens.

Availability of Data and Materials

The datasets used and analyzed during the current study are available from the corresponding author on reasonable request.

Author Contributions

WG collected and analyzed whole-genome data, collected experimental data, drafted the initial manuscript, and prepared the figures. BZ collected experimental data. ZY collected mouse blood and organ/tissue samples and collated the experimental data. CC analyzed the experimental data. FY contributed to conception and supervision

of the study, critical review and important revision of the manuscript, obtaining funding for the present study. All authors contributed to editorial changes in the manuscript. All authors read and approved the final manuscript. All authors have participated sufficiently in the work and agreed to be accountable for all aspects of the work.

Ethics Approval and Consent to Participate

All animal experiments were approved by the Animal Experimentation Ethics Committee of Tongji Medical College (Approval No. 4704) on April 6, 2025, and were conducted in accordance with the National Institutes of Health Guide for the Care and Use of Laboratory Animals.

Acknowledgment

We would like to thank the Animal Experiment Center of Tongji Medical College, Huazhong University of Science and Technology, for providing the experimental platform.

Funding

This research was funded by the National Key R&D Program of China (Nos.2022YFC2704204).

Conflict of Interest

The authors declare no conflicts of interest.

Declaration of AI and AI-Assisted Technologies in the Writing Process

During the preparation of this work, the authors used ChatGPT (OpenAI, San Francisco, CA, USA) to assist with translation and to check spelling and grammar. After using this tool, the authors reviewed and edited the content as needed and take full responsibility for the content of the publication.

References

[1] Song KW, Lim M, Monje M. Complex neural-immune interactions shape glioma immunotherapy. Immunity. 2025; 58: 1140–1160. https://doi.org/10.1016/j.immuni.2025.04.017.

[2] Wang W, Li T, Cheng Y, Li F, Qi S, Mao M, *et al*. Identification of hypoxic macrophages in glioblastoma with therapeutic potential for vasculature normalization. Cancer Cell. 2024; 42: 815–832.e12. https://doi.org/10.1016/j.ccell.2024.03.013.

[3] Tsien CI, Pugh SL, Dicker AP, Raizer JJ, Matuszak MM, Lallana EC, *et al*. NRG Oncology/RTOG1205: A Randomized Phase II Trial of Concurrent Bevacizumab and Reirradiation Versus Bevacizumab Alone as Treatment for Recurrent Glioblastoma. Journal of Clinical Oncology: Official Journal of the American Society of Clinical Oncology. 2023; 41: 1285–1295. https://doi.org/10.1200/JCO.22.00164.

[4] Zhang M, Zhu J, Bao Y, Ao Q, Mao X, Qiu Z, *et al*. Bevacizumab in ovarian cancer therapy: current advances, clinical challenges, and emerging strategies. Frontiers in Bioengineering and Biotechnology. 2025; 13: 1589841. https://doi.org/10.3389/fbioe.2025.1589841.

[5] Li B, Xu D, Zhou J, Wang SC, Cai YX, Li H, *et al*. Monitoring Bevacizumab-Induced Tumor Vascular Normalization by Intravoxel Incoherent Motion Diffusion-Weighted MRI. Journal of Magnetic Resonance Imaging: JMRI. 2022; 56: 427–439. https://doi.org/10.1002/jmri.28012.

[6] Zhong L, Gan L, Wang B, Wu T, Yao F, Gong W, *et al*. Hyperacute rejection-engineered oncolytic virus for interventional clinical trial in refractory cancer patients. Cell. 2025; 188: 1119–1136.e23. https://doi.org/10.1016/j.cell.2024.12.010.

[7] Long L, Gao J, Zhang R. PTTG1 Enhances Oncolytic Adenovirus 5 Entry into Pancreatic Adenocarcinoma Cells by Increasing CXADR Expression. Viruses. 2023; 15: 1153. https://doi.org/10.3390/v15051153.

[8] Guo J, Xiong S, Zhang X, Gong W, Si Y, Ma D, *et al*. Preclinical Efficacy and Safety of an Oncolytic Adenovirus KD01 for the Treatment of Bladder Cancer. Pharmaceuticals (Basel, Switzerland). 2025; 18: 511. https://doi.org/10.3390/ph18040511.

[9] Ren F, Narita R, Rashidi AS, Fruhwürth S, Gao Z, Bak RO, *et al*. ER stress induces caspase-2-tBID-GSDME-dependent cell death in neurons lytically infected with herpes simplex virus type 2. The EMBO Journal. 2023; 42: e113118. https://doi.org/10.15252/embj.2022113118.

[10] Dai Z, Si Y, Xiong S, Li Y, Ye J, Gao Q, *et al*. Chimeric Ad5/35 oncolytic adenovirus overcome preexisting neutralizing antibodies and enhance tumor targeting efficiency. Cancer Gene Therapy. 2025; 32: 418–436. https://doi.org/10.1038/s41417-025-00884-x.

[11] Xie Y, Yang F, He L, Huang H, Chao M, Cao H, *et al*. Single-cell dissection of the human blood-brain barrier and glioma blood-tumor barrier. Neuron. 2024; 112: 3089–3105.e7. https://doi.org/10.1016/j.neuron.2024.07.026.

[12] Kurdi M, Bamaga A, Alkhotani A, Alsharif T, Abdel-Hamid GA, Selim ME, *et al*. Mitochondrial DNA Alterations in Glioblastoma and Current Therapeutic Targets. Frontiers in Bioscience (Landmark Edition). 2024; 29: 367. https://doi.org/10.31083/j.fbl2910367.

[13] Cerretti G, Bosio A, Librizzi G, Pintacuda G, Caccese M, Salvalaggio A, *et al*. Bevacizumab in recurrent glioblastoma: does dose matter? Our monocentric and comparative experience. Journal of Neuro-oncology. 2025; 173: 449–456. https://doi.org/10.1007/s11060-025-04992-4.

[14] Beylerli O, Gareev I, Kaprin A, Ahmad A, Chekhonin V, Yang S, *et al*. Hemorrhagic and ischemic risks of anti-VEGF therapies in glioblastoma. Cancer Gene Therapy. 2025; 32: 762–777. https://doi.org/10.1038/s41417-025-00914-8.

[15] Nowacka A, Śniegocki M, Smuczyński W, Bożiłow D, Ziółkowska E. Angiogenesis in Glioblastoma-Treatment Approaches. Cells. 2025; 14: 407. https://doi.org/10.3390/cells14060407.

[16] Ma R, Li Z, Chiocca EA, Caligiuri MA, Yu J. The emerging field of oncolytic virus-based cancer immunotherapy. Trends in Cancer. 2023; 9: 122–139. https://doi.org/10.1016/j.trecan.2022.10.003.

[17] He T, Hao Z, Lin M, Xin Z, Chen Y, Ouyang W, *et al*. Oncolytic adenovirus promotes vascular normalization and non-classical tertiary lymphoid structure formation through STING-mediated DC activation. Oncoimmunology. 2022; 11: 2093054. https://doi.org/10.1080/2162402X.2022.2093054.

[18] Wang M, Chen Y, Tian L, Wu C, Chen J, Hu J, *et al*. Vascular Normalization Augments the Antitumor Efficacy of Combined HDAC Inhibitor with Immunotherapy in Solid Tumors. Cancer Discovery. 2025; 15: 1883–1904. https://doi.org/10.1158/2159-8290.CD-24-1033.

[19] Jacob F, Salinas RD, Zhang DY, Nguyen PTT, Schnoll JG, Wong SZH, *et al*. A Patient-Derived Glioblastoma Organoid Model and Biobank Recapitulates Inter- and Intra-tumoral Heterogeneity. Cell. 2020; 180: 188–204.e22. https://doi.org/10.1016/j.cell.2019.11.036.

[20] Swamy K. Vascular normalization and immunotherapy: Spawning a virtuous cycle. Frontiers in Oncology. 2022; 12: 1002957. https://doi.org/10.3389/fonc.2022.1002957.

[21] Guo G, Zhang Z, Zhang J, Wang D, Xu S, Liu G, *et al*. Predicting recurrent glioblastoma clinical outcome to immune checkpoint inhibition and low-dose bevacizumab with tumor in situ fluid circulating tumor DNA analysis. Cancer Immunology, Immunotherapy: CII. 2024; 73: 193. https://doi.org/10.1007/s00262-024-03774-7.

[22] Chen Y, Chen X, Bao W, Liu G, Wei W, Ping Y. An oncolytic virus-T cell chimera for cancer immunotherapy. Nature Biotechnology. 2024; 42: 1876–1887. https://doi.org/10.1038/s41587-023-02118-7.